Purification and Characterization of Two Monomeric Kinesin Constructs†

Michele L. Moyer,‡ Susan P. Gilbert,§ and Kenneth A. Johnson*,‡

Department of Biochemistry and Molecular Biology, 106 Althouse Laboratory, Pennsylvania State University, University Park, Pennsylvania 16802, and Department of Biological Sciences, 215 Clapp Hall, University of Pittsburgh, Pittsburgh, Pennsylvania 15260

Received January 3, 1996; Revised Manuscript Received March 22, 1996⊗

ABSTRACT: Steady-state and pre-steady-state kinetic methods were used to analyze two shorter *Drosophila* kinesin constructs (K341 and K366) in comparison to K401. K341, K366, and K401 represent the kinesin motor domains containing the N-terminal 341, 366, or 401 amino acids, respectively. K401 is dimeric ($K_d = 37 \pm 17$ nM) whereas both K366 and K341 are monomeric [Correia *et al.* (1995) *Biochemistry 34,* 4898−4907]. Like native kinesin and K401, K341 and K366 demonstrate low ATPase activity in the absence of microtubules (0.03 and 0.01 s^{-1}, respectively), and ADP release is rate-limiting during steady-state turnover. Microtubules activate the steady-state ATPase to 84 s^{-1} for K341 ($K_{m,ATP} = 100$ μM; $K_{0.5,MT} = 3.2$ μM tubulin) and 64 s^{-1} for K366 ($K_{m,ATP} = 65$ μM; $K_{0.5,MT} = 2.5$ μM tubulin) in comparison to K401 at 20 s^{-1} ($K_{m,ATP} = 60$ μM; $K_{0.5,MT} = 1$ μM tubulin). The rapid quench experiments for all three constructs show a burst of product formation during the first turnover, indicating the rate-limiting step for the microtubule-activated ATPase occurs after ATP hydrolysis. The interaction of K341 and K366 with the microtubule was analyzed by electron microscopy. The results show that K341 and K366, like K401, bind to the microtubule with an 8 nm axial periodicity. However, the addition of K366 to microtubules resulted in significant aggregation of microtubules. The pre-steady-state kinetic results show that K341 retains the kinetic and structural properties necessary to compare directly the kinetic properties of monomeric and dimeric kinesins, although the microtubule-activated ATPase is significantly faster for the monomeric constructs, suggesting possible interactions in the dimer which inhibit ATP turnover as part of the coupling to force production.

Members of the kinesin superfamily are related by sequence similarity within an approximately 340 amino acid region [reviewed by Vale and Goldstein (1990) and Bloom and Endow (1994)]. This conserved region contains both the ATP and microtubule binding sites and is therefore thought to constitute the minimal mechanochemical motor domain of conventional kinesin and the kinesin-like proteins (Yang *et al.*, 1990). Native kinesin is a tetrameric protein composed of two identical heavy chains (110−140 kDa) and two identical light chains (60−80 kDa) (Bloom *et al.*, 1988; Kuznetsov *et al.*, 1988). Sequence analysis suggests that the heavy chains are made up of an N-terminal motor domain, an extended α-helical coiled-coil domain, and a small globular carboxy-terminal domain (Yang *et al.*, 1989). Evidence of interaction between the two motor domains has been suggested by both *in vitro* motility assays and biochemical studies (Hackney, 1994a; Howard *et al.*, 1989; Gilbert *et al.*, 1995; Block *et al.*, 1990).

In motility assays, native kinesin is observed to track microtubule protofilaments as it moves by 8 nm steps toward the plus-end of microtubules (Svoboda *et al.*, 1993; Ray *et al.*, 1993; Gelles *et al.*, 1988). Because single molecules of native kinesin have been observed to move loads over distances of several micrometers (Svoboda & Block, 1994; Howard *et al.*, 1989), kinesin is defined as a processive enzyme. Berliner and colleagues have examined one-headed (K340-BIO) and two-headed (K401-BIO and K441-BIO) biotinated kinesin derivatives in motility assays (Berliner *et al.*, 1995). Although a single dimeric kinesin molecule can produce movement, a high surface density of monomeric kinesin on the coated beads is required. The mean velocity of K401-BIO movement is approximately 610 nm s^{-1} while K340-BIO moves at approximately 170 nm s^{-1}. Moreover, although dimeric kinesin was observed to track microtubule protofilaments as it progressed toward the plus-end of the microtubule, monomeric kinesin molecules (at high surface density on the beads) appeared to lose this tracking ability, such that K340-BIO was observed to wander over the entire accessible surface of the microtubule. These findings provide some support of a model of kinesin movement, in which one head remains tightly bound to the microtubule while the other detaches from the microtubule and moves forward (Hackney, 1994a; Howard *et al.*, 1989; Gilbert *et al.*, 1995; Block *et al.*, 1990). However, it has not been shown that a single molecule of one-headed kinesin is capable of supporting concerted movement. Moreover, in the absence of a detailed biochemical analysis of the shorter kinesin constructs, it is not possible to conclude that the defective motion is simply attributable to the monomeric quaternary structure of the kinesin and not due to other defects resulting from truncation of the C-terminus of the head domain.

We have expressed in *Escherichia coli* three truncated mutants of the *Drosophila* kinesin heavy chain. K341, K366, and K401 each represent the kinesin motor domain containing the N-terminal 341, 366, or 401 amino acids, respectively.

† This work is supported by grants to K.A.J. (GM26726 from the National Institutes of Health) and M.L.M. (Training Grant GM08358 from the National Institutes of Health).

* Author to whom correspondence should be addressed. Telephone: (814) 865-1200. Fax: (814) 865-3030. Email: Kaj@ecl.psu.edu.

‡ Pennsylvania State University.

§ University of Pittsburgh.

⊗ Abstract published in *Advance ACS Abstracts,* May 1, 1996.

S0006-2960(96)00017-7 CCC: $12.00

The quaternary structure of these proteins has been determined by sedimentation velocity and sedimentation equilibrium centrifugation (Correia *et al.*, 1995). K401 has been shown to be dimeric ($K_d = 37 \pm 17$ nM), yet K341 and K366 are monomeric. K341 is monomeric up to at least 10 μM, and K366 is monomeric up to 4 μM total protein concentration. These results indicate that the amino acids located within positions 367 and 401 are involved in the formation of the dimer interface.

K401 has been shown to exhibit kinetic characteristics expected of native kinesin (Gilbert & Johnson, 1993). Pre-steady-state experiments with K401 have resulted in a mechanism that accounts for the processivity of dimeric kinesin. Processivity can be defined biochemically as the number of ATP molecules hydrolyzed per encounter of kinesin with the microtubule (Gilbert *et al.*, 1995). Experiments performed with K401 have demonstrated processive ATP hydrolysis by kinesin. The kinetic analysis of monomeric kinesin will test directly models proposed from the kinetic studies with dimeric kinesin and clarify the role of interactions between the kinesin heads in force production.

EXPERIMENTAL PROCEDURES

Materials. Expression vector pET-5b and *Escherichia coli* cell line HMS174(DE3) were obtained from Novagen Inc. (Madison, WI). *E. coli* cell line DH5α was from Gibco BRL (Gaithersburg, MD). Restriction enzymes were purchased from New England Biolabs, Inc. (Beverly, MA), and the Gene Clean kit was from Bio101 (La Jolla, CA). BioRex 70 resin (wet bead size 75−150 μm) was purchased from BioRad Laboratories (Richmond, CA), and DEAE Sepharose FF was from Pharmacia LKB (Uppsala, Sweden). Taxol was obtained from CalBiochem (La Jolla, CA), and poly(ethylenimine) (PEI) was purchased from Aldrich Chemical Co. (Milwaukee, WI). Radiolabeled ATP ([α-^{32}P]ATP, >3000 Ci/mmol) was from ICN Biomedicals, Inc. (Costa Mesa, CA). Phosphocreatine and phosphocreatine kinase (250 units/mg) were obtained from Sigma Chemical Co. (St. Louis, MO). PEI−cellulose F TLC plates (EM Separations of E. Merck, 20 × 20 cm, plastic backed) were obtained from VWR Scientific (Pittsburgh, PA).

Media and Buffers. The following media and buffers were used for the experiments described: Miller LB broth (10 g of bacto tryptone, 5 g of bacto yeast extract, and 10 g of NaCl per liter); lysis buffer (50 mM Tris-HCl, pH 7.8, 2.5 mM EDTA, 1 mM DTT, 100 mM NaCl, and 5 mM PMSF); ATPase buffer (50 mM HEPES, pH 7.2 with KOH, 5 mM magnesium acetate, 0.1 mM EDTA, 0.1 mM EGTA, 50 mM potassium acetate, and 1 mM DTT); buffer A (50 mM Tris-HCl, pH 7.4, 0.1 mM EDTA, 1 mM DTT, 20 μM ATP, and 5 mM $MgCl_2$); buffer B (50 mM Tris-HCl, pH 7.8, 0.1 mM EDTA, 1 mM DTT, 20 μM ATP, and 5 mM $MgCl_2$); PM buffer (100 mM Pipes, pH 6.7, 5 mM magnesium acetate, and 1 mM EGTA). The pH of all buffers was adjusted at the temperature at which they were used.

pET5b-K341 and pET5b-K366 Construction. pET5b-K341 and pET5b-K366 refer to the plasmids constructed from expression vector pET5b (Rosenberg *et al.*, 1987; Studier *et al.*, 1990) and from the truncated kinesin genes which encode the N-terminal 341 and 366 amino acids of the *Drosophila* kinesin heavy chain (Yang *et al.*, 1989). Polymerase chain reaction (Saiki *et al.*, 1988) was used to construct the plasmids. Template DNA was isolated from plasmid pET5b-K401 (Gilbert & Johnson, 1993) which contains a truncated kinesin gene encoding the N-terminal 401 amino acids of the *Drosophila* kinesin heavy chain (Yang *et al.*, 1989). Oligonucleotides were chemically synthesized using the Applied Biosystems 380A synthesizer (Pennsylvania State University Biotechnology Institute, University Park, PA). For K341 and K366, the 5′-PCR oligonucleotide (5′-GGAGATATACATATGGCTAGCCG GGAACGAGAG-3′) contained an *Nhe*I site and corresponds to four amino acid residues of the pET5b vector and seven N-terminal amino acid residues of the parent clone pET5b-K401(Yang *et al.*, 1989). For K341, the 3′-PCR oligonucleotide (5′-AACGTGGTCTGCGTTAACTAGGATCCTAC-TGCCGAGGAA-3′) consisted of 18 bases corresponding to residues 336−341 of pET5b-K401 (Yang *et al.*, 1989) followed by a stop codon and a *Bam*HI site. Twelve bases corresponding to amino acids 345−348 of pET5b-K401 (Yang *et al.*, 1989) were added to enhance annealing of primer to template DNA. For K366, the 3′-PCR oligonucleotide (5′-GCCCGACTAAAGGG TAAGTAGGATCCGCTG-GAGATCGAGCTT-3′) consisted of 18 bases corresponding to amino acids 361−366 of pET5b-K401, followed by a stop codon and *Bam*HI site. Fifteen bases corresponding to amino acids 370−374 of pET5b-K401 (Yang *et al.*, 1989) were added to enhance annealing of primer to template DNA. The PCR conditions during amplification were those suggested by Perkin-Elmer Cetus (Norwalk, CT) with the following temperature cycle: 94 °C (2 min), 45 °C (1 min), and 72 °C (3 min) for 25 cycles.

The pET5b vector was digested with *Nhe*I and *Bam*HI and treated with alkaline phosphatase. The digested vector and PCR products were purified by agarose gel electrophoresis and recovered using a Gene Clean kit. The PCR products were ligated into the pET5b vector using T4 DNA ligase. The products of the ligation reactions were used to transform *E. coli* strain DH5α. Plasmid DNA isolated from these cells was subjected to restriction mapping with *Nhe*I and *Bam*HI. Clones containing the insert gene were identified by agarose gel electrophoresis. Plasmids from these clones were used to transform *E. coli* strain HMS174(DE3). In this expression system, expression of the truncated kinesin protein was under the control of the T7 promoter with T7 RNA polymerase induced by IPTG (Studier & Moffatt, 1986; Rosenberg *et al.*, 1987; Studier *et al.*, 1990). The N-termini of the resulting proteins are the same as the N-terminus of the kinesin heavy chain. K341 terminates at Asn341. Its molecular mass is 37 825 Da as calculated from the amino acid sequence. K366 terminates at Lys366. Its molecular mass is 40 955 Da as calculated from the amino acid sequence.

Expression of K341 and K366. Single colonies were selected and grown at 37 °C to an A_{600} of 0.4−0.6 in LB supplemented with 0.1 mg/mL ampicillin. This initial culture was used to inoculate (at 1:100) a 2 L culture of LB plus 0.1 mg/mL ampicillin and shaken at 37 °C to an A_{600} of 0.4−0.6. The 2 L culture was used to inoculate 230 L of LB plus ampicillin (0.05 mg/mL) in a BioService 300 L fermentor (BioService, Inc., Bethlehem, PA). Fermentation was continued at 37 °C for 4 h. The temperature was then shifted to 20 °C and induced with IPTG (final concentration 75 μM). Fermentation was continued for 12 h at 20 °C. Cells were harvested by centrifugation (Sharples AS-16

Supercentrifuge rotor, 16 800 rpm, feed-rate 1 L/min; Sharples Division, Alfa-Laval Separation, Inc., Warminster, PA). Approximately 500 g of *E. coli* was obtained from 230 L of LB. Cells were frozen as aliquots in liquid nitrogen and stored at −80 °C.

Purification of K341. All purification steps were performed at 4 °C or on ice. Sixty grams of cells was diluted to final volume of 300 mL (1 g/5 mL) in lysis buffer plus lysozyme at 0.2 mg/mL and incubated on ice for 60 min with stirring. Cells were lysed by four cycles of freezing (with liquid N_2) and thawing (37 °C). The extract was then centrifuged (Sorvall SS34 rotor, 18 000 rpm, 40 min). The supernatant was decanted and stored at 4 °C. Pellets were resuspended in 100 mL of lysis buffer, homogenized using a Wheaton glass tissue grinder, and centrifuged (SS34 rotor, 18 000 rpm, 30 min). The resulting supernatant was combined with the first supernatant. PEI was added to a final concentration of 0.35% and stirred on ice for 30 min. The extract was then adjusted to 0.4 M NaCl and stirred 20 min on ice. The extract was centrifuged (GSA rotor, 8000 rpm, 10 min), and the PEI pellet was discarded. The supernatant was adjusted to 5 mM $MgCl_2$ and 30 μM ATP and dialyzed against 2 × 6 L of buffer A with 25 mM NaCl.

On the second day of the purification, the dialysate was clarified (Beckman 60 Ti rotor, 40 000 rpm, 60 min). Clarified supernatant was then loaded at 4 mL/min onto a 400 mL BioRex 70 column (12.5 cm^2 × 32 cm) equilibrated with buffer A plus 25 mM NaCl. The column was washed with equilibration buffer at 4 mL/min until the A_{280} returned to base line. A 5 column-volume gradient from 25 mM to 500 mM NaCl at a flow rate of 5 mL/min was used to elute K341 from the column. Fractions were analyzed by SDS−PAGE. K341 eluted at approximately 300 mM NaCl. Fractions enriched in K341 were pooled and dialyzed against 2 × 6 L of buffer B with 10 mM NaCl.

On day 4, the dialysate was clarified (Beckman 45 Ti rotor, 40 000 rpm, 60 min) and loaded at 2 mL/min onto a 25 mL DEAE Sepharose column (12.5 cm × 2 cm^2) equilibrated with buffer B plus 10 mM NaCl. The column was washed with equilibration buffer until the A_{280} returned to base line. A 5 column-volume gradient from 10 mM NaCl to 50 mM NaCl at 2 mL/min was used to elute K341. Fractions were analyzed by SDS−PAGE. K341 eluted at approximately 20 mM NaCl.

On day 5, fractions enriched in K341 were pooled and concentrated by Amicon Ultrafiltration (Model 8050 stirred cell with YM10 membrane; Danvers, MA) to 3−4 mL. K341 was then dialyzed against 4 L of ATPase buffer for 2−3 h and clarified by centrifugation (Beckman 50 Ti rotor, 40 000 rpm, 60 min), and aliquots were frozen in liquid N_2. Protein was stored at −80 °C. The procedure yields approximately 20 mg of K341 at >99% purity by SDS−PAGE.

Purification of K366. Purification of K366 was carried out as described above for K341 with exceptions as follow: The cell extract was dialyzed against buffer A plus 150 mM NaCl, and the BioRex 70 column was equilibrated with buffer A with 150 mM NaCl. After the clarified extract was loaded, the column was washed with equilibration buffer until the A_{280} returned to base line. A 5 column-volume gradient from 150 mM to 500 mM NaCl was then employed to elute the protein from the column. K366 eluted from the BioRex column at approximately 400 mM NaCl. A DEAE Sepharose column was equilibrated with buffer B with 10 mM NaCl. A 5 column-volume gradient from 10 mM to 50 mM NaCl was used to elute the protein from the column. K366 eluted from the DEAE column at approximately 20 mM NaCl. The procedure yields approximately 20 mg of K366 at >99% purity by SDS−PAGE.

SDS−PAGE. SDS−PAGE was performed using 8% acrylamide/2 M urea slab gels with 3% stacking gels according to the buffer formulations of Laemmli (1970) and stained with Coomassie brilliant blue R-250 (Fairbanks *et al.*, 1971). The molecular mass standards used were rabbit muscle phosphorylase *b* (97 kDa), BSA (66 kDa), hen egg white ovalbumin (43 kDa), bovine carbonic anhydrase (31 kDa), and soybean trypsin inhibitor (21 kDa) (BioRad Laboratories).

Kinesin Active-Site Titrations. After truncation of the kinesin heavy chain to the N-terminal 341 or 366 amino acids, no tryptophan residues are present in K341, and only one tryptophan residue remains in K366. Because the majority of the absorbance of the protein at 280 nm is due to tryptophan residues (Edelhoch, 1967), protein concentration was not determined spectrophotometrically. Rather, estimates were obtained by use of the Bradford assay (Bradford, 1976), and then actual active-site concentrations were determined by measurement of the concentration of ADP bound to kinesin using the phosphocreatine kinase assay described below.

Phosphocreatine Kinase Coupled Enzyme Assay. The concentration of active monomeric kinesin and the rate of ADP release from kinesin in the absence of microtubules were determined using a coupled enzyme assay. In the assay, creatine kinase is used to convert free ADP to ATP. Conversion of [α-^{32}P]ADP to [α-^{32}P]ATP then provided a measurement of ADP release from kinesin. The assay was first tested to be sure the rate of ATP synthesis under the conditions used was sufficiently fast to measure the ADP release rate of kinesin. First, [α-^{32}P]ADP was produced by incubating [α-^{32}P]ATP with 2 N HCl at 95 °C for 2.5 min. Hydrolyzed [α-^{32}P]ATP was then neutralized with 2 M Tris−3 M NaOH. The reaction was then initiated by mixing 0.30 mg/mL creatine kinase and 4 mM phosphocreatine (5 μL total volume) with 50 μM [α-^{32}P]ADP (5 μL total volume). The reaction was incubated at 25 °C and sampled from 0 to 3 min. The reaction was terminated with 10 μL of 2 N HCl, followed by addition of 20 μL of chloroform, and neutralization with 5 μL of 2 M Tris−3 M NaOH. An aliquot (1.5 μL) of each sample was spotted onto a PEI−cellulose TLC plate. The plate was developed with 0.6 M KH_2PO_4, pH 3.4, and radiolabeled ATP and ADP were quantified using a Betascope 603 blot analyzer (Betagen, Waltman, MA). The data were fit to a single exponential by nonlinear regression using KaleidaGraph (Synergy Software, Reading, PA). The rate of ATP synthesis was determined to be 0.25 ± 0.01 s^{-1} at the conditions of the reaction (data not shown). This rate is approximately 10 times the anticipated rate of ADP release from kinesin in the absence of microtubules (Gilbert & Johnson, 1993; Huang & Hackney, 1994). Therefore, in the presence of unlabeled MgATP, the assay could be used to determine the rate of ADP release from K341 and K366.

In the activity assay, the total kinesin concentration was first estimated by Bradford assay (Bradford, 1976) using BSA as a standard. K341 or K366 (10−25 μM by Bradford assay, 50 μL volume) was then incubated with [α-^{32}P]ATP (20−

50 μM, 50 μL volume) for 10 min at 25 °C in ATPase buffer. This incubation allows ADP at the active-site to be exchanged with [α-^{32}P]ATP which is then hydrolyzed to [α-^{32}P]-ADP and held at the enzyme site. The reaction was initiated by mixing 5 μL of labeled kinesin with 20 μL of chase solution containing 0.30 mg/mL phosphocreatine kinase and 4 mM phosphocreatine in ATPase buffer with or without 5 mM MgATP. Reactions were sampled from 0 to 8 min. The reactions were terminated with 25 μL of 2 N HCl, followed by addition of 50 μL of chloroform. The sample was then neutralized with 12 μL of 2 M Tris−3 M NaOH. Zero time points were determined as follows: an aliquot of labeled kinesin (5 μL) was mixed with 5 μL of 2 N HCl, and 20 μL of chase solution was mixed with 20 μL of 2 N HCl; the denatured proteins were then mixed together; and 50 μL of chloroform and 12 μL of 2 M Tris−3 M NaOH were added. An aliquot (1.5 μL) of each sample was spotted onto a PEI−cellulose TLC plate. The plate was developed in 0.6 M potassium phosphate buffer, pH 3.4. Radiolabeled ATP and ADP were quantified using a Betascope 603 blot analyzer.

In the presence of excess nonradioactive MgATP, a decrease in radioactive [α-^{32}P]ADP was observed as the ADP was released from kinesin and then converted to ATP by creatine kinase. The data were fit to a single exponential function [product = $A \exp(-k_1 t) + C$] to determine the rate (k_1) of ADP release and amplitude (A) of the reaction which defines the active-site concentration. In the absence of unlabeled MgATP, the [α-^{32}P]ADP was released from kinesin and converted to [α-^{32}P]ATP by phosphocreatine kinase, which then bound back to the kinesin and was hydrolyzed. In this way, the concentration of [α-^{32}P]ADP should remain constant and is equal to the concentration of active kinesin sites in the reaction if the release of ADP from kinesin is the slowest step in the cycle of ATP hydrolysis by kinesin. However, because the rate of ATP synthesis was only 10-fold faster than the rate of ADP release, a transient reduction in [α-^{32}P]ADP was observed which is attributable to the attainment of the steady-state balance between hydrolysis and synthesis of ATP. In this case, the data were fit to a single exponential as described above. The sum of the amplitude (A) and constant term (C) of the exponential function is equal to the active-site concentration. The active-site concentrations determined in the presence and absence of unlabeled MgATP were averaged. All concentrations reported in figure legends and text are final active-site concentrations after mixing kinesin with the reactants.

Mammalian Brain Tubulin and Microtubules. Bovine brain microtubules were prepared by two cycles of temperature-dependent polymerization and depolymerization (Shelanski *et al.*, 1973; Sloboda *et al.*, 1976), and tubulin was separated from microtubule-associated protein by the method of Borisy *et al.* (1974) as modified by Omoto and Johnson (1986). On the day of each experiment, an aliquot of tubulin was thawed, diluted to 10−15 mg/mL protein with PM buffer, adjusted to 1 mM GTP, and cold-depolymerized for 30 min on ice. The tubulin was then centrifuged (microfuge, 14 000 rpm, 15 min, 4 °C) to sediment aggregates. The supernatant was adjusted to 20 μM taxol and incubated at 34 °C for 10 min to polymerize the microtubules. The microtubules were then diluted in PM buffer plus 20 μM taxol to dilute the GTP concentration to 0.1 mM and stabilize the microtubules. The preparation was incubated for an additional 20 min at 34 °C followed by centrifugation (SS34 rotor, 18 000 rpm, 20 min, 25 °C). The microtubule pellet was resuspended in ATPase buffer plus 20 μM taxol, and the protein concentration was determined by the Schacterie and Pollack (1973) modification of Lowry *et al.* (1951).

Scheme 1

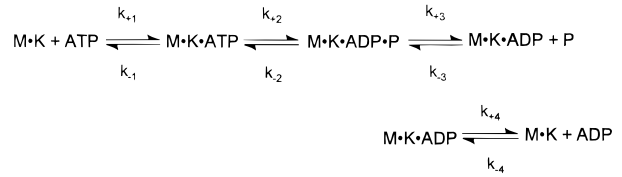

Steady-State ATPase Assays. ATPase measurements were made by following the hydrolysis of [α-^{32}P]ATP to form product [α-^{32}P]ADP as described previously (Gilbert & Johnson, 1993). In the absence of microtubules, the reaction times sampled were from 0 to 20 min. In the presence of microtubules, the reaction times sampled were from 0 to 75 s. Concentrations reported in figure legends are final concentrations after mixing reactants. The concentration dependence of the observed rate was fit to a hyperbola by nonlinear regression using KaleidaGraph (Synergy Software, Reading, PA) to determine the steady-state kinetic constants.

Rapid Quench Experiments. The ATPase assays were performed at 25 °C in ATPase buffer using a KinTek chemical quench flow instrument (KinTek Corp., State College, PA) (Johnson, 1983) as described previously (Gilbert & Johnson, 1994). Data were modeled using the KINSIM kinetic simulation program (Barshop *et al.*, 1983). Curves were fit to the mechanism shown in Scheme 1 and were modeled by setting the acid quench output equal to the sum of K·ADP·P plus K·ADP and ADP. Numerical integration using the KINSIM program used an iterative process to obtain the best fit taking into account the concentrations of enzyme and MgATP.

Electron Microscopy. The microtubule·kinesin complex was formed at room temperature with 1 μM K341 or K366 and 1 μM microtubules (tubulin heterodimer) in ATPase buffer. After incubation for 5 min, protein solutions were placed on carbon- and formvar-coated grids. Grids were then negatively stained with 2% uranyl acetate and examined by transmission electron microscopy (JEOL 1200 EX-II).

RESULTS

Purification of K341 and K366. Figure 1 shows representative samples from the purification of K341 as described under Experimental Procedures. The purified K341 migrates at approximately 38 kDa in this gel system, which is in close agreement with the molecular mass (37 825 Da) calculated from the amino acid sequence. Purified K366 migrates at approximately 41 kDa, which is in agreement with the calculated molecular mass (40 955 Da). Note that K366 comigrates with a 41 kDa *E. coli* protein which is removed from kinesin by BioRex 70 chromatography. Furthermore, the BioRex 70 column resolves the truncated kinesin constructs from the majority of other *E. coli* proteins because the kinesin constructs are among the few proteins that bind to the resin under the conditions used. Comparison of lane g (the second 18 K pellet) and lane h (the soluble protein after lysis) shows that approximately 50−60% of the K341 present in the cells remains insoluble. This is consistent with

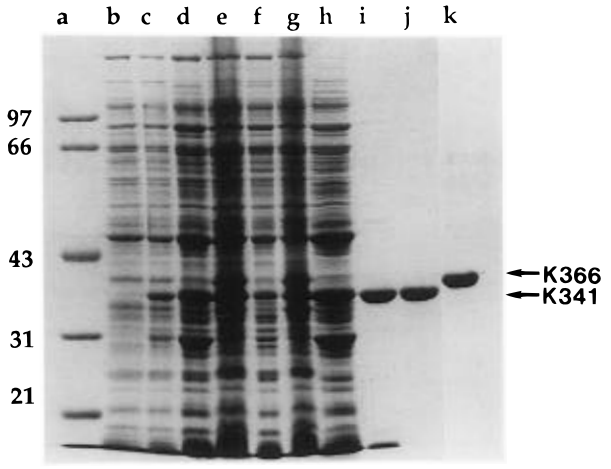

FIGURE 1: Protein purification. An 8% acrylamide/2 M urea gel stained with Coomassie R-250 showing all steps in the purification of K341. Lane a, standards; lane b, preinduced cell lysate; lane c, induced cell lysate; lane d, first 18K supernatant; lane e, first 18K pellet; lane f, second 18K supernatant; lane g, second 18K supernatant; lane h, 0.4 M NaCl supernatant following PEI precipitation; lane i, K341-enriched fractions following BioRex 70 chromatography. Each sample was loaded in equal volumes to determine relative concentrations of K341. Lane j, purified K341 (~5 μg); lane k, purified K366 (~5 μg).

what is observed during the purification of K366 and K401 (Gilbert & Johnson, 1993). Approximately 25 mg of K341 or K366 has been purified consistently from 60 g of cell paste.

Active-Site Determination. The concentration of active-sites and the ADP release rate of K341 and K366 were determined using a coupled enzyme assay in which K341 or K366 with [α-^{32}P] ADP bound was mixed with creatine kinase and phosphocreatine in the presence or absence of excess nonradioactive MgATP (see Figure 2). In the presence of excess unlabeled MgATP, the [α-^{32}P]ADP that is released from kinesin is converted to [α-^{32}P]ATP, and so the loss of [α-^{32}P]ADP with time defines the kinetics of ADP release from the kinesin. A fit of the data to a single exponential (see Experimental Procedures) yields the rate of release and the amplitude of the reaction which defines the active-site concentration. In a parallel experiment in the absence of excess unlabeled MgATP, a steady-state balance is achieved between the release of [α-^{32}P]ADP from kinesin and its conversion to [α-^{32}P]ATP by creatine kinase, followed by its hydrolysis once again to [α-^{32}P]ADP by kinesin. In this way, one expects the concentration of [α-^{32}P]ADP to remain constant at a value equal to the concentration of kinesin active-sites present in the reaction mixture (see Figure 2). However, to account for a small transient observed after the addition of creatine kinase, the data were fit to a single exponential [product = $A \exp(-k_1 t) + C$], and the sum of the amplitude (A) and the constant term (C) from the fit of the data was used to define the active-site concentration by extrapolation to zero time. The active-site concentrations determined in the presence and absence of nonradioactive MgATP were averaged. By Bradford assay (BSA standard), the concentrations of K341 or K366 were 147 μM or 238 μM, respectively. The active concentrations of K341 and K366 were determined to be 136 μM and 165 μM, respectively. The percentage of active K341 and K366 was consistent between two different protein preparations of both K341 and K366. In each subsequent experiment described, the concentration of kinesin specified is the active-site concentration.

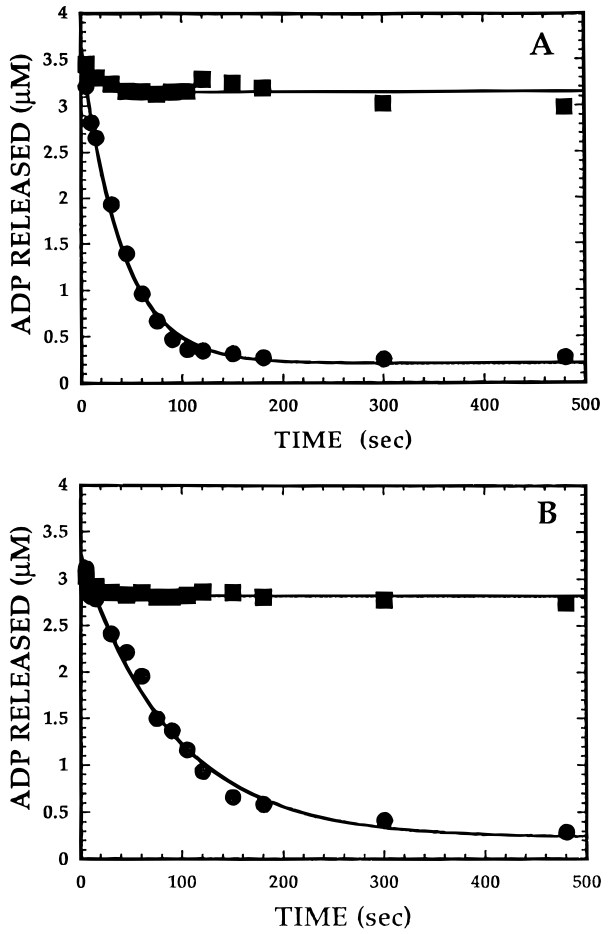

FIGURE 2: Active-site determination and ADP release in the absence of microtubules. (A) 4.1 μM K341 or (B) 5 μM K366 with bound [α-^{32}P]ADP was rapidly mixed with 0.30 mg/mL creatine kinase, 4 mM phosphocreatine with (●) or without (■) 5 mM MgATP at 25 °C. In the absence of MgATP, the concentration of active kinesin was determined. The data were fit to a single exponential [product = $A \exp(-k_1 t) + C$]. The sum of the amplitude (A) and the constant term (C) from the single exponential equation is equal to the ADP concentration in the reaction. The ADP concentration is equal to the concentration of active K341 or K366 in the reaction. For K341, the concentration of active-site was determined to be 3.53 ± 0.18 μM. For K366, the active-site concentration was 3.13 ± 0.13 μM. In the presence of MgATP, the rate of ADP release (k_1) was determined. The data were fit to a single exponential with the rate of ADP release 0.033 ± 0.001 s^{-1} for K341 and 0.017 ± 0.002 s^{-1} for K366. Under these conditions, the amplitude of the single exponential is equal to active kinesin in the reaction. In the presence of unlabeled MgATP, the amplitude was 3.45 ± 0.07 μM for K341 and 3.03 ± 0.09 μM for K366. The active-site concentration determined in the absence of MgATP and the concentration determined in the presence of MgATP were averaged to give the final active-site concentration.

The rate of ADP release for K341 is 0.03 s^{-1} and for K366 is 0.01 s^{-1} (Figure 2). K341 and K366 both demonstrate the low ATPase rate in the absence of microtubules (0.02 s^{-1} and 0.01 s^{-1}, respectively), similar to what has been reported for native kinesin and other truncated kinesin constructs. Furthermore, ADP release is rate-limiting in the absence of microtubules as has been reported previously (Hackney *et al.*, 1989; Sadhu & Taylor, 1992; Gilbert & Johnson, 1993; Hackney, 1994b; Huang & Hackney, 1994; Lockhart *et al.*, 1995; Ma & Taylor, 1995a).

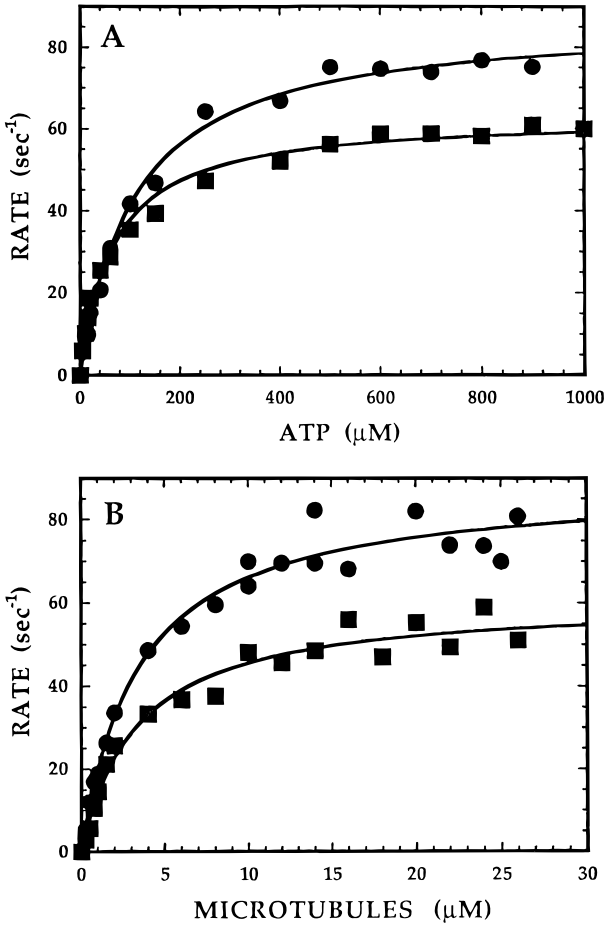

FIGURE 3: Steady-state ATP hydrolysis activity of K341 and K366. (A) 0.08 μM K341 (●) or 0.13 μM K366 (■) was incubated with microtubules (14 μM tubulin for K341; 16 μM tubulin for K366) and MgATP (0−0.9 mM for K341; 0−1 mM for K366) at 25 °C. The rate of ATP hydrolysis is shown as a function of ATP concentration. The data were fit to a hyperbola. For K341, k_{cat} = 84 ± 4 s^{-1} and $K_{m,ATP}$ = 100 ± 13 μM. For K366, k_{cat} = 68 ± 6 s^{-1} and $K_{m,ATP}$ = 65 ± 4 μM. (B) 0.74 μM K341 (●) or 0.5 μM K366 (■) was incubated with 2 mM MgATP and microtubules (0−28 μM tubulin) at 25 °C. In the absence of microtubules, the rate of ATP hydrolysis for K341 is 0.019 ± 0.005 s^{-1} and for K366, 0.010 ± 0.007 s^{-1}. The rate of ATP hydrolysis is shown as a function of tubulin concentration. The data were fit to a hyperbola. For K341, k_{cat} = 84 ± 5 s^{-1} and $K_{0.5,MT}$ = 3.2 ± 0.1 μM. For K366, k_{cat} = 60 ± 1 s^{-1} and $K_{0.5,MT}$ = 2.5 ± 0.7 μM.

Steady-State ATPase Activity. Steady-state experiments in the presence of microtubules have been performed for both K341 and K366. Like native kinesin and K401, both K341 and K366 show a dramatic increase in the rate of ATP hydrolysis in the presence of microtubules (Gilbert & Johnson, 1993). For K341, microtubules activate ATP turnover from 0.02 s^{-1} in the absence of microtubules to 84 s^{-1} at saturating concentrations of ATP and microtubules ($K_{m,ATP}$ = 100 μM; $K_{0.5,MT}$ = 3.2 μM tubulin). For K366, microtubules activate steady-state ATPase from 0.01 s^{-1} to 64 s^{-1} ($K_{m,ATP}$ = 64 μM; $K_{0.5,MT}$ = 2.5 μM tubulin) (Figure 3). In comparison, microtubules activate K401 from 0.01 s^{-1} to 20 s^{-1} ($K_{m,ATP}$ = 62 μM; $K_{0.5,MT}$ = 1 μM tubulin) (Gilbert *et al.*, 1995).

Rate of ATP Hydrolysis. Pre-steady-state kinetic analysis of microtubule-activated K341 and K366 was used in order to determine the rate of ATP hydrolysis at the active-site of these enzymes. The microtubule·kinesin complex was first formed with 28 μM microtubules (tubulin heterodimer) and

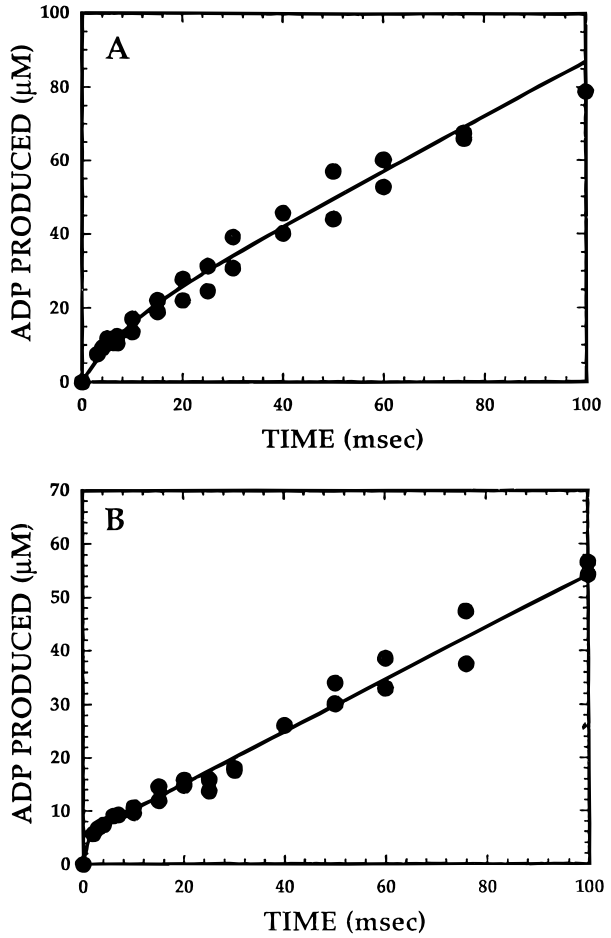

FIGURE 4: Pre-steady-state kinetics of ATP hydrolysis. Preformed (A) M·K341 complex or (B) M·K366 complex (11 μM kinesin, 14 μM tubulin) was reacted with 400 μM [α-^{32}P]MgATP (final concentrations after mixing in rapid quench) for 3−200 ms followed by acid quench. The curves were calculated by numerical integration according to the mechanism in Scheme 1. The following rate constants were calculated for K341: k_{+1} = 3.6 μM^{-1} s^{-1}, k_{-1} = 819 s^{-1}, k_{+2} > 300 s^{-1}, k_{+3} = 134 s^{-1}, and k_{+4} = 300 s^{-1}. For K366, the rate constants were k_{+1} = 24 μM^{-1} s^{-1}, k_{-1} = 376 s^{-1}, k_{+2} > 300 s^{-1}, k_{+3} = 77 s^{-1}, and k_{+4} = 300 s^{-1}.

22 μM kinesin (twice the final concentrations achieved after mixing in rapid quench). A concentration of 14 μM microtubules was sufficient to maximally activate the steady-state ATPase of K341 and K366. The M·K complex was then rapidly mixed with 400 μM MgATP (final concentration) in the rapid quench instrument. Figure 4 shows the time course of ADP formation for K341 and K366. The kinetics of ATP hydrolysis show a pre-steady-state burst for both K341 and K366. The initial fast rate of product formation (the burst) corresponds to the first turnover of the enzyme which was followed by a slower rate of product formation (the linear phase) corresponding to steady-state turnover of K341 or K366. The observation of a pre-steady-state burst in the rapid quench experiments indicates that the rate-limiting step in the ATPase pathway occurs after ATP hydrolysis. A burst of product formation was observed previously in rapid quench experiments performed with K401, at a rate of ~100 s^{-1} at 400 μM MgATP (Gilbert & Johnson, 1994). For monomeric kinesin constructs, at the conditions tested, the burst rate is faster than can accurately be measured using the rapid quench instrument. For both K341 and K366, the burst rate was >300 s^{-1}, at least 3-fold faster than was observed for dimeric K401, although it is

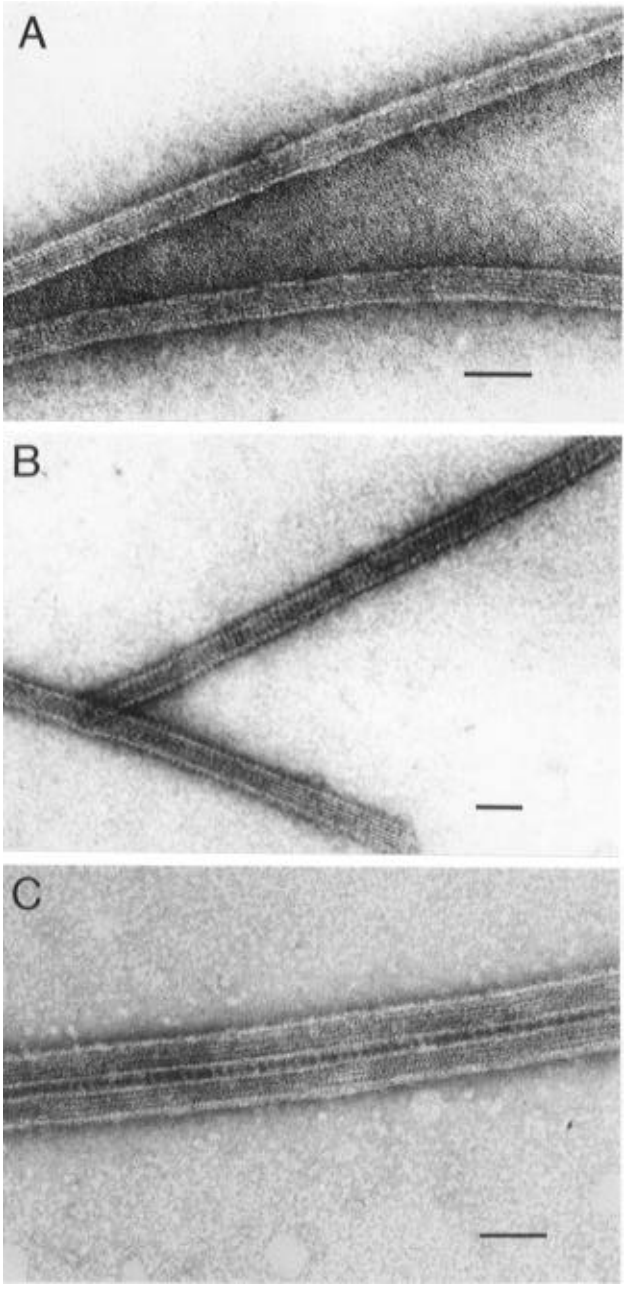

FIGURE 5: Electron micrographs of microtubules in the presence or absence of K341 or K366. Microtubules were incubated with K341 or K366 at a molar ratio of 1 kinesin molecule per tubulin heterodimer and examined by electron microscopy. Panel A, microtubules; panels B and C, microtubules decorated with K341 and K366, respectively. K341 is observed to bind to the microtubule with an axial periodicity of 8.3 ± 2 nm (average of 22 measurements of K341 bound to 6 different microtubules). K366 is observed to bind with a regular periodicity of 7.9 ± 2 nm (average of 10 measurements of K366 bound to 4 different microtubules). Scale bar is 50 nm.

difficult to measure these rates accurately since the shortest time point attainable in the quench-flow instrument is 3 ms.

Microtubule−Kinesin Complex. Electron microscopy was used to examine the interaction of the monomeric kinesin constructs with the microtubule surface. The microtubule·kinesin complex was formed with K341 and K366 in the absence of nucleotide. K341 was observed to bind the outer surface of the microtubule with an axial repeat of ~8 nm, supporting the interpretation of one kinesin motor domain per tubulin heterodimer (Figure 5B). These results are consistent with the 8 nm periodicity observed for decoration of microtubules by truncated kinesin constructs from *Drosophila* (K401, DKH340, and DKH392) and mouse (K340) (Harrison *et al.*, 1993; Huang *et al.*, 1994; Kikkawa *et al.*, 1995). K366 was also observed to bind to the microtubule with an axial repeat of ~8 nm. However, by light microscopy (data not shown), K366 was observed to cause extensive bundling of microtubules. Electron microscopy confirmed that K366 causes microtubules to be cross-linked by K366 (Figure 5C).

DISCUSSION

In work done to date, monomeric constructs, K341 and K366, show similarities to dimeric K401. All of the constructs demonstrate a low ATPase activity that is limited by the rate of ADP release in the absence of microtubules (Gilbert & Johnson, 1993). In the presence of microtubules, the rate-limiting step in the ATPase pathway of each of the constructs analyzed occurs after ATP hydrolysis (Gilbert & Johnson, 1994) and in the case of K401 has been shown to correspond to the rate of kinesin release from the microtubule during the force-producing cycle (Gilbert *et al.*, 1995). Similarities observed show that monomeric constructs retain the structural conformation necessary to compare the kinetic properties of monomeric and dimeric constructs. However, the differences observed between monomeric and dimeric constructs are of greater interest. Two differences of note have been observed. First, it was observed that the microtubule-activated ATPase activity is greater for the monomeric constructs than for the dimeric K401 (Gilbert & Johnson, 1993). This large increase in activity suggests that ATP hydrolysis may be partially uncoupled from force production for single-headed kinesins (Stewart *et al.*, 1993) and that coupling between heads of the dimer inhibits ATP turnover. This coupling may make a significant contribution to the pathway of force production. Second, K366 has been observed to cause extensive cross-linking of microtubules. The bundling of microtubules may be due to aggregation of K366, which may be a function of the weak self-association of kinesin C-terminal tail fragments lined up along the microtubules. Alternatively, microtubules may be cross-linked by an interaction of the C-terminus of K366 directly with the microtubule surface. No bundling of microtubules was evident with the M·K341 complex. Because of the additional complications caused by microtubule bundling, further studies toward understanding cooperativity between the motor domains of kinesin cannot be performed using monomeric K366.

The steady-state characterization of other monomeric and dimeric kinesin constructs has been reported. Huang and Hackney (Huang & Hackney, 1994; Hackney, 1994b) have characterized truncated kinesin constructs from *Drosophila*: DKH392, which is dimeric; and DKH340, a monomeric kinesin protein. The $K_{0.5,MT}$ values determined for DKH392 and DKH340 are 50 and 160 nM, respectively, significantly lower that those determined for K401 or K341. This difference may be due to different salt concentrations in the buffer systems used in the assays. The reported k_{cat} value for DKH340 is 80 s^{-1}, which is in close agreement with the k_{cat} value determined here for K341. However, the reported k_{cat} value of DKH392 is 45 s^{-1}, significantly faster than that observed for K401 at 20 s^{-1}. This difference may be due to the concentration of DKH392 used in the steady-state assay. In these experiments, DKH392 was used at 8.4

nM. Dimeric kinesin constructs have been observed to undergo reversible dissociation at concentrations below the K_d for dimer dissociation (Correia *et al.*, 1995). Measurements of the K_d of dimeric *Drosophila* K401 (37 nM) predict that K401 would be predominantly monomeric at 8.4 nM. Dissociation of dimeric kinesin may be responsible, in part, for the fast steady-state rate observed for DKH392.

Steady-state characterization of recombinant truncated kinesin constructs from rat (Lockhart *et al.*, 1995) and human sources (Ma & Taylor, 1995b) has also been reported. Rat K401 and human HK379 kinesin constructs are both dimeric. The k_{cat} values and $K_{0.5,MT}$ values for both constructs are consistent with steady-state constants determined for K401 from *Drosophila* (Gilbert & Johnson, 1993). Lockhart *et al*. (1995) have also reported steady-state values for rat K340, a monomeric kinesin protein. For rat K340, $K_{0.5,MT}$ is 4 μM and k_{cat} is 39 s^{-1}. Although the $K_{0.5,MT}$ value for rat K340 is in close agreement with that of *Drosophila* K341 reported here, the steady-state rate for rat K340 is only approximately half that of *Drosophila* K341. This difference may be due to different assay conditions, different sources of recombinant kinesin protein, or different methods of determining the concentration of truncated kinesin present in the reaction. The steady-state ATPase rates reported here were calculated based on active-site concentrations of kinesin in the reaction. The concentration of rat K340 was determined spectrophotometrically.

Although reported kinetic constants vary, an overall trend in k_{cat} and $K_{0.5,MT}$ values has been observed when comparing monomeric and dimeric kinesin constructs. The k_{cat} values for the microtubule-activated ATPase of monomeric constructs are elevated compared to those of dimeric kinesin constructs, and the $K_{0.5,MT}$ values for monomeric constructs are increased relative to the dimeric kinesins. Additionally, several studies have reported motility rates for monomeric and dimeric kinesin constructs (Stewart *et al.*, 1993; Berliner *et al.*, 1995). Again, although reported motility rates vary, the overall trend is that motility rates are slower for monomeric constructs than for dimeric constructs. The motility data are consistent with the suggestion that for monomeric constructs ATP hydrolysis is uncoupled from force production. Furthermore, the results suggest that formation of dimeric kinesin is required for the characteristic processivity of kinesin.

A model of ordered sequential release of each head of dimeric kinesin has been proposed based upon transient state kinetic studies with dimeric K401 (Gilbert *et al.*, 1995). The data suggest that the two heads differ when bound to the microtubule such that only one of the two heads is poised to release after ATP binds. We are in the process of testing this model using K341 as a kinetically independent kinesin motor domain. Comparison of the unique differences observed in kinetic studies between monomeric and dimeric kinesin may help to define the mechanistic and structural basis of cooperativity and processivity of kinesin in motility and kinetic assays. Two features of the kinesin ATPase mechanism are proposed to account for the observed processivity: (1) fast rebinding of kinesin to the microtubule and (2) ordered sequential release and rebinding of the two heads of kinesin to the microtubule. In motility assays, kinesin is immobilized on a glass coverslip or is attached to a relatively large bead. In either case, kinesin is far less diffusible than when it is free in solution. Low or negligible diffusibility of kinesin may promote attachment of the motor domain to the microtubule, thereby allowing movement of monomeric kinesin to be observed even if sequential release and reattachment by two motor domains are normally required to promote motility.

Ongoing work involving transient state kinetic experiments with K341 will help to establish if sequential release of the two kinesin motor domains is required for processive ATP hydrolysis or if fast rebinding of kinesin to the microtubule is sufficient for processivity. The present study defines the basic kinetic and structural features of two monomeric kinesin constructs to provide the foundation for further analysis. Moreover, the unusual properties of the monomeric kinesins call into question the use of these kinesins as simple monomeric counterparts of the full-length kinesin. In particular, the increased microtubule-activated ATPase activity and the tendency of the longer length monomer to cause bundling of microtubules suggest significant interaction between kinesin motor domains in the dimer. It is likely that the region between 341 and 401 amino acids is involved in formation of the dimer interface and in transmission of information from one kinesin head to its partner involved in coordinating the activities of the two heads.

ACKNOWLEDGMENT

We thank Wayne Kaboord of the Pennsylvania State University Biotechnology Institute's Electron Microscope Facility for his assistance in obtaining the electron micrographs.

REFERENCES

Barshop, B. A., Wrenn, R. F., & Frieden, C. (1983) *Anal. Biochem. 130*, 134−145.
Berliner, E., Young, E. C., Anderson, K., Mahtani, H. K., & Gelles, J. (1995) *Nature 373*, 718−721.
Block, S. M., Goldstein, L. S. B., & Schnapp, B. J. (1990) *Nature 348*, 348−352.
Bloom, G. S., & Endow, S. A. (1994) *Protein Profile 1*, 1106−1116.
Bloom, G. S., Wagner, M. C., Pfister, K. K., & Brady, S. T. (1988) *Biochemistry 27*, 3409−3416.
Borisy, G. G., Olmstead, J. B., Marcum, J. M., & Allen, C. (1974) *Fed. Proc., Fed. Am. Soc. Exp. Biol. 33*, 167−174.
Bradford, M. M. (1976) *Anal. Biochem. 72*, 248−254.
Correia, J. J., Gilbert, S. P., Moyer, M. L., & Johnson, K. A. (1995) *Biochemistry 34*, 4898−4907.
Edelhoch, H. (1967) *Biochemistry 6*, 1948−1954.
Fairbanks, G., Steck, T. L., & Wallach, D. F. H. (1971) *Biochemistry 10*, 2606−2617.
Gelles, J., Schnapp, B. J., & Sheetz, M. P. (1988) *Nature 331*, 450−453.
Gilbert, S. P., & Johnson, K. A. (1993) *Biochemistry 32*, 4677−4684.
Gilbert, S. P., & Johnson, K. A. (1994) *Biochemistry 33*, 1951−1960.
Gilbert, S. P., Webb, M. R., Brune, M., & Johnson, K. A. (1995) *Nature 373*, 671−676.
Hackney, D. D. (1994a) *Proc. Natl. Acad. Sci. U.S.A. 91*, 6865−6869.
Hackney, D. D. (1994b) *J. Biol. Chem. 269*, 16508−16511.
Hackney, D. D., Malik, A.-S., & Wright, K. W. (1989) *J. Biol. Chem. 264*, 15943−15948.
Harrison, B. C., Marchese-Ragona, S. P., Gilbert, S. P., Cheng, N., Steven, A. C., & Johnson, K. A. (1993) *Nature 362*, 73−75.
Howard, J., Hudspeth, A. J., & Vale, R. D. (1989) *Nature 342*, 154−158.
Huang, T. G., & Hackney, D. D. (1994) *J. Biol. Chem. 269*, 16493−16501.

Huang, T. G., Suhan, J., & Hackney, D. D. (1994) *J. Biol. Chem. 269*, 16502−16507.
Johnson, K. A. (1983) *J. Biol. Chem. 258*, 13825−13832.
Kikkawa, M., Ishikawa, T., Wakabayashi, T., & Hirokawa, N. (1995) *Nature 376*, 274−277.
Kuznetsov, S. A., Vaisberg, E. A., Shanina, N. A., Magretova, N. N., Chernyak, V. Y., & Gelfand, V. I. (1988) *EMBO J. 7*, 353−356.
Laemmli, U. K. (1970) *Nature (London) 227*, 680−685.
Lockhart, A., Crevel, I. M.-T. C., & Cross, R. A. (1995) *J. Mol. Biol. 249*, 763−771.
Lowry, O. H., Rosebrough, N. J., Farr, A. L., & Randall, R. J. (1951) *J. Biol. Chem. 193*, 265−275.
Ma, Y. Z., & Taylor, E. W. (1995a) *Biochemistry 34*, 13233−13241.
Ma, Y. Z., & Taylor, E. W. (1995b) *Biochemistry 34*, 13242−13251.
Okada, Y., Yamazaki, H., Sekine-Aizawa, Y., & Hirokawa, N. (1995) *Cell 81*, 769−780.
Omoto, C. K., & Johnson, K. A. (1986) *Biochemistry 25*, 419−427.
Ray, S., Meyhofer, E., Milligan, R. A., & Howard, J. (1993) *J. Cell Biol. 121*, 1083−1093.
Rosenberg, A. H., Lade, B. N., Chui, D., Lin, S., Dunn, J. J., & Studier, F. W. (1987) *Gene 56*, 125−135.
Sadhu, A., & Taylor, E. W. (1992) *J. Biol. Chem. 267*, 11352−11359.
Saiki, R. K., Gelfand, D. H., Stoffel, S., Scharf, S. J., Higuchi, R., Horn, G. T., Mullis, K. B., & Erlich, H. A (1988) *Science 239*, 487−491.
Schacterle, G. R., & Pollack, R. L. (1973) *Anal. Biochem. 51*, 654−655.
Shelanski, M. L., Gaskin, F., & Cantor, C. R. (1973) *Proc. Natl. Acad. Sci. U.S.A. 70*, 765−768.
Sloboda, R. D., Dentler, W. L., & Rosenbaum, J. L. (1976) *Biochemistry 15*, 4497−4505.
Stewart, R. J., Thaler, J. P., & Goldstein, L. S. (1993) *Proc. Natl. Acad. Sci. U.S.A. 90*, 5209−5213.
Studier, F. W., & Moffatt, B. A. (1986) *J. Mol. Biol. 189*, 113−130.
Studier, F. W., Rosenberg, A. H., Dunn, J. J., & Dubendorff, J. W. (1990) *Methods Enzymol. 185*, 60−89.
Svoboda, K., & Block, S. M. (1994) *Cell 77*, 773−784.
Svoboda, K., Schmidt, C. F., Schnapp, B. J., & Block, S. M. (1993) *Nature 365*, 721−727.
Vale, R. D., & Goldstein, L. S. B. (1990) *Cell 60*, 883−885.
Yang, J. T., Laymon, R. A., & Goldstein, L. S. (1989) *Cell 56*, 879−889.
Yang, J. T., Saxton, W. M., Stewart, R. J., Raff, E. C., & Goldstein, L. S. B. (1990) *Science 249*, 42−47.

BI960017N